



## Early View

Research letter

# Analysis of pathological changes of the epithelium in the COVID-19 patient airways

Wenguang Yin, Weitao Cao, Guangde Zhou, Lifei Wang, Jing Sun, Airu Zhu, Zhongfang Wang, Yumin Zhou, Xiaoqing Liu, Yimin Li, Nanshang Zhong, Jincun Zhao, Lei Liu, Pixin Ran

Please cite this article as: Yin W, Cao W, Zhou G, *et al.* Analysis of pathological changes of the epithelium in the COVID-19 patient airways. *ERJ Open Res* 2021; in press (<https://doi.org/10.1183/23120541.00690-2020>).

This manuscript has recently been accepted for publication in the *ERJ Open Research*. It is published here in its accepted form prior to copyediting and typesetting by our production team. After these production processes are complete and the authors have approved the resulting proofs, the article will move to the latest issue of the ERJOR online.

©The authors 2021. This version is distributed under the terms of the Creative Commons Attribution Non-Commercial Licence 4.0. For commercial reproduction rights and permissions contact [permissions@ersnet.org](mailto:permissions@ersnet.org)

## **Analysis of pathological changes of the epithelium in the COVID-19 patient airways**

Wenguang Yin<sup>1,4</sup>, Weitao Cao<sup>1,4</sup>, Guangde Zhou<sup>2,4</sup>, Lifei Wang<sup>3,4</sup>, Jing Sun<sup>1,4</sup>, Airu Zhu<sup>1</sup>, Zhongfang Wang<sup>1</sup>, Yumin Zhou<sup>1</sup>, Xiaoqing Liu<sup>1</sup>, Yimin Li<sup>1</sup>, Nanshang Zhong<sup>1</sup>, Jincun Zhao<sup>1</sup>, Lei Liu<sup>2</sup> and Pixin Ran<sup>1</sup>

<sup>1</sup>State Key Laboratory of Respiratory Disease, National Clinical Research Center for Respiratory Disease, Guangzhou Institute of Respiratory Health, the First Affiliated Hospital of Guangzhou Medical University, Guangzhou, Guangdong, 510182, P.R. China.

<sup>2</sup>Shenzhen Key Laboratory of Pathogen and Immunity, National Clinical Research Center for Infectious Disease, State Key Discipline of Infectious Disease, Shenzhen Third People's Hospital, Second Hospital Affiliated to Southern University of Science and Technology, Shenzhen, China.

<sup>3</sup>Department of Radiology, National Clinical Research Center for Infectious Disease, Third People's Hospital, Second Hospital Affiliated to Southern University of Science and Technology, Shenzhen, China.

<sup>4</sup>These authors contributed equally: Wenguang Yin, Weitao Cao, Guangde Zhou, Lifei Wang, Jing Sun.

Correspondence: Pixin Ran, [pxran@gzhmu.edu.cn](mailto:pxran@gzhmu.edu.cn) or Lei Liu, [liulei3322@aliyun.com](mailto:liulei3322@aliyun.com)

To the editor,

The outbreak of severe acute respiratory syndrome coronavirus 2 (SARS-CoV-2) has caused more than 70 million infections and approximately 1.6 million deaths worldwide<sup>1</sup>. However, the pathological changes in the COVID-19 airways remain unclear due to limited accessibility of autopsy or biopsy.

Here, we report for one of the first pathological changes of the epithelium in the severe COVID-19 patient airways. The COVID-19 lungs exhibited much MUC5AC-containing mucus accumulation in many bronchioles. The number of mucus-producing goblet cells was dramatically increased, and the number of multiciliated cells and bronchiolar club cells was significantly reduced. IL-13 levels were also dramatically increased in the COVID-19 lungs. The levels of secretoglobin CC16 secreted by club cells were significantly reduced in 9 COVID-19 patients. Furthermore, SARS-CoV-2 nucleocapsid proteins were detected in human airway epithelial cells after *in vitro* infection.

A 66-year-old man from Shenzhen, Guangdong Province, China, traveled to Wuhan on December 29, 2019 and returned to Shenzhen on January 04, 2020. He was admitted to the hospital on January 11, 2020 with clinical symptoms of cough, fever, myalgia and mild dyspnea. He was a non-smoker with the comorbidity of hypertension. SARS-CoV-2 infection was identified by performing a real-time reverse transcriptase-polymerase-chain-reaction (RT-PCR) assay for a nasopharyngeal swab specimen<sup>2</sup>. Noninvasive ventilation and mechanical ventilation were administered to him on January 11, 2020 and January 20, 2020, respectively. After admission to the intensive care unit (ICU) on January 25, 2020, he developed respiratory failure, received lung transplantation therapy on February 25, 2020, and was declared clinically dead on February 26, 2020. On chest X-rays, we observed multiple patchy shadows with a progressive increase in areas in his lungs from January 12 to January 22 (Fig. A1-C1). Chest CT showed bilateral and peripheral ground-glass opacities associated with intralobular septal thickening in his lungs on January 13 (Fig. D1, E1). Lesions in his lungs increased in extent with obvious heterogeneous density and air bronchogram on January 23 (Fig. F1, G1). On January 30, his lungs exhibited a dramatic decrease in brightness with much more patchy shadows (Fig. H1). From February 01, the brightness of his lungs was further decreased with a large area of patchy shadow (Fig. I1, J1). Samples from the injured lungs of this patient were embedded in paraffin and sectioned for examination.

To test pathological changes in COVID-19 airways, we analyzed lung sections by histological staining. The COVID-19 patient lungs exhibited severe hemorrhage in the airways and alveoli (Fig. K1). Many of the COVID-19 distal bronchioles were plugged by mucus, accompanied by goblet cell hyperplasia in the airway epithelium (Fig. L1). To examine cellular changes in COVID-19 airways, we performed a detailed analysis of the airway epithelium in healthy controls and the patient by immunostaining<sup>3</sup>. We observed that many of the distal bronchioles including the smaller ones in the COVID-19 patient were plugged by MUC5AC-containing mucus (Fig. M1, N1, P1, Q1). MUC5AC<sup>+</sup> goblet cells mainly localize in bronchi and are barely detectable in distal bronchioles in humans<sup>4</sup>. In

contrast, a large number of MUC5AC<sup>+</sup> goblet cells were observed in more than half of the bronchioles including the smaller ones in the COVID-19 patient compared to healthy controls (Fig. M1, O1, P1, R1). *MUC5AC* mRNA levels were dramatically increased in the COVID-19 lungs compared to healthy controls by a quantitative reverse transcription PCR assay (Fig. A2). MUC5B is required for mucociliary clearance in the airways<sup>5</sup>. Notably, MUC5B protein and mRNA levels appeared to be dramatically reduced in the airway epithelium in the COVID-19 patient compared to healthy controls (Fig. B2-D2). Multiciliated cells beat to constantly propel mucus from the distal to proximal airways for clearance of mucus-trapped pathogens and particles<sup>6</sup>. The number of acetylated alpha-tubulin<sup>+</sup> multiciliated cells appeared to be significantly reduced in the small bronchioles in the COVID-19 patient (Fig. E2, F2).

Club cells secrete CC16, a secretoglobin that can attenuate airway mucus production and hypersecretion<sup>7-9</sup>. We observed that the number of CC16<sup>+</sup> club cells was significantly reduced in distal bronchioles in the COVID-19 patient compared to healthy controls (Fig. G2, H2). CC16 mRNA levels appeared to be dramatically reduced in the lungs of the COVID-19 patient (Fig. I2). Next, we examined circulating CC16 levels in serum from 7 healthy non-smoking controls aged 38-67 years and 9 severe COVID-19 patients aged 41-72 years including 4 smokers by ELISA. CC16 levels were significantly decreased in COVID-19 patients compared to healthy controls (Fig. J2). In humans, IL-13 can induce mucus production in the lungs<sup>10,11</sup>. IL-13 levels appeared to be dramatically increased in COVID-19 patients compared to healthy controls (Fig. K2, L2).

To investigate whether human airway epithelial cells are susceptible to SARS-CoV-2, we used primary bronchial epithelial cells cultured *in vitro* at air-liquid interface (ALI) as a model of human airway epithelium formation<sup>12</sup>. After a 14-day differentiation (Fig. M2, N2), we performed a 24-hour virus inoculation into human airway epithelium at a multiplicity of infection (MOI) of 0.2, SARS-CoV-2 nucleocapsid proteins were detected in human airway epithelial cells by immunostaining (Fig. O2), indicating that the human airway epithelium is a potential site for SARS-CoV-2 infection.

## Discussion

This study provides one of the first description of pathological changes in the COVID-19 airway epithelium. The COVID-19 airways are plugged by abundant MUC5AC-containing mucus, accompanied by hyperplasia of goblet cells as well as hypoplasia of club cells and multiciliated cells. It is possible that SARS-CoV-2 infection causes impaired airway epithelial cell homeostasis, leading to mucus overproduction and/or hypersecretion and/or accumulation, ultimately resulting in bronchiole obstruction, dyspnea or even death. These findings warn that COVID-19 patients with dyspnea and mucus plugs in the airways should be treated with caution. It is possible that the forced airflow from mechanical ventilation pushes mucus into the alveoli, which may dramatically reduce the air-exchange surface in the lungs and result in more severe hypoxia. Thus, we propose that mucus in the airways should be examined and removed before using mechanical ventilation for COVID-19 patients.

Decreased CC16 levels have been shown to be associated with pulmonary diseases with mucus overproduction, including COPD<sup>13,14</sup> and asthma<sup>15</sup>. CC16 could inhibit mucus production and hypersecretion in mouse airways and the ALI differentiation model of HBE cells<sup>7-9</sup>. IL-13 promotes mucus production in the lungs<sup>10,11</sup>. Our findings that severe COVID-19 patients exhibit decreased CC16 levels and increased IL-13 levels, reveal other possible causes of airway mucus accumulation in COVID-19 patients.

### **Acknowledgements**

We thank Ruiting Sun for imaging assistance.

### **Ethics approval**

This study was approved by the Ethics Committee of the First Affiliated Hospital of Guangzhou Medical University (No. 2020-51). Because of the urgent need to collect data on this emerging infectious disease, the requirement for written informed consents were waived.

### **Author contributions**

W.Y. and P.R. conceived the project, designed experiments, and analyzed data; W.C., L.L, G.Z., L.W. and J.S. contributed to experiments and data analysis; W.Y., Z.W., Y.Z., N.Z., and J.Z. contributed to discussion and data analysis; A.Z., X.L. and Y.L. contributed to patient recruitment and sample collection. W.Y. and P.R. wrote the manuscript. This study was supported by the grant Guangdong Key Research and Development Project (2020B1111330001).

### **Disclosures**

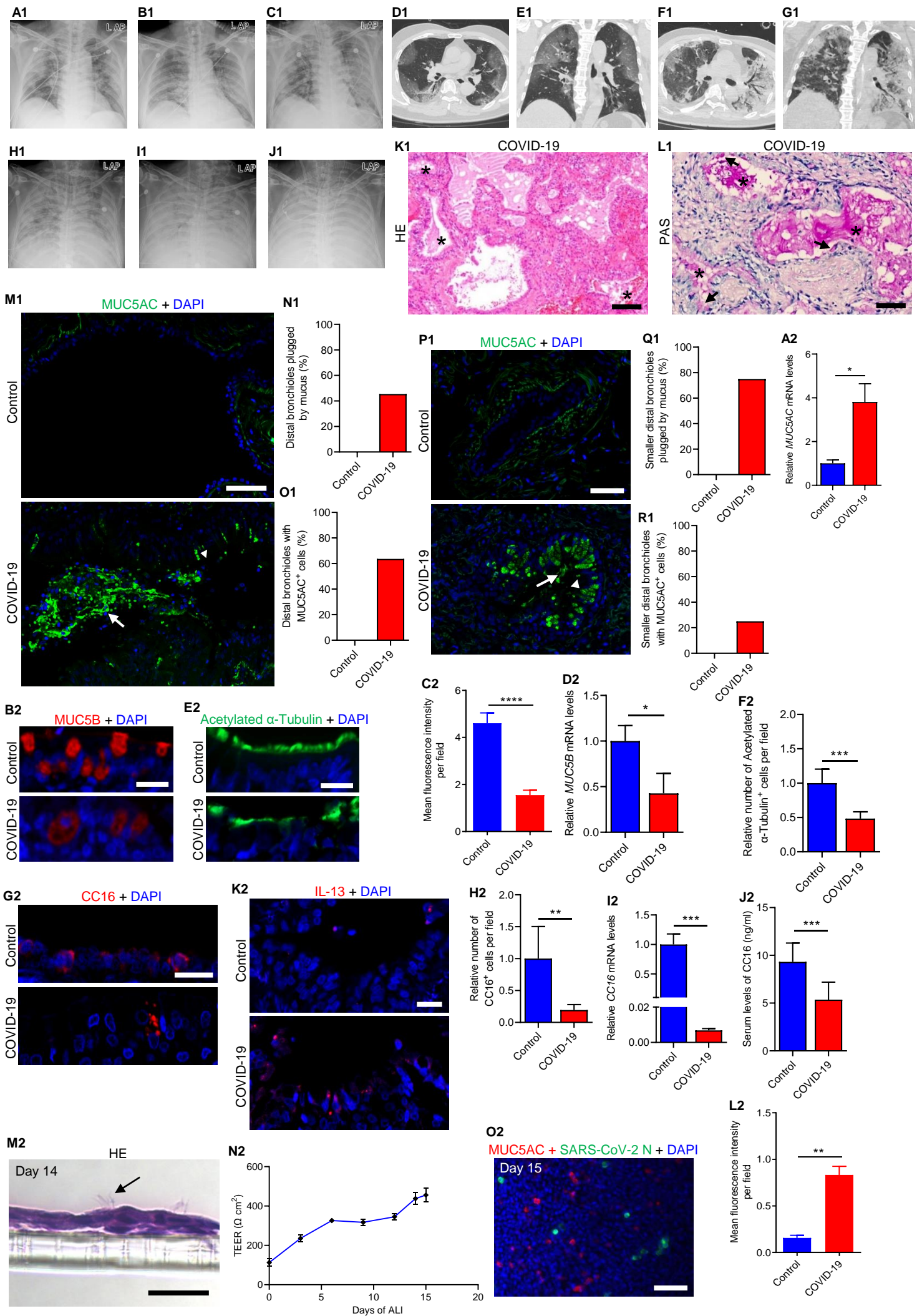
Authors have disclosed no conflicts of interest.

### **References**

1. World Health Organization. Weekly epidemiological update - 15 December 2020. <https://www.who.int/publications/m/item/weekly-epidemiological-update---15-december-2020>.
2. Wang, D. et al. Clinical Characteristics of 138 Hospitalized Patients With 2019 Novel Coronavirus-Infected Pneumonia in Wuhan, China. *JAMA*. 323, 1061-1069 (2020).
3. Yin, W. et al. The potassium channel KCNJ13 is essential for smooth muscle cytoskeletal organization during mouse tracheal tubulogenesis. *Nat Commun*. 9: 2815 (2018).
4. Okuda, K. et al. [Localization of Secretory Mucins MUC5AC and MUC5B in Normal/Healthy Human Airways](#). *Am J Respir Crit Care Med*. **199**, 715-727 (2019).
5. Roy, M.G. et al. [Muc5b is required for airway defence](#). *Nature*. **505**, 412-6 (2014).
6. Bustamante-Marin, X.M. & Ostrowski, L E. [Cilia and Mucociliary Clearance](#). *Cold Spring Harb Perspect Biol*. **9**, pii: a028241 (2017).
7. Wang, S.Z. et al. [CCSP modulates airway dysfunction and host responses in an Ova-challenged mouse model](#). *Am J Physiol Lung Cell Mol Physiol*. **281**, L1303-11 (2001).
8. Tokita, E., Tanabe, T., Asano, K., Suzaki, H. & Rubin, B.K. [Club cell 10-kDa protein attenuates airway mucus hypersecretion and inflammation](#). *Eur Respir J*. **44**, 1002-10 (2014).
9. Laucho-Contreras, M.E. et al. [Protective role for club cell secretory protein-16 \(CC16\) in the development of COPD](#). *Eur Respir J*. **45**, 1544-56 (2015).
10. Miotto, D. et al. Interleukin-13 and -4 expression in the central airways of smokers with chronic bronchitis. *Eur Respir J*. **22**, 602-8 (2003).
11. Alevy, Y.G. et al. IL-13-induced airway mucus production is attenuated by MAPK13 inhibition. *J Clin Invest*. 122, 4555-68 (2012).
12. Schmid, A. et al. Modulation of Wnt signaling is essential for the differentiation of ciliated epithelial cells in human airways. *FEBS Lett*. **591**, 3493-3506 (2017).
13. Lomas, D.A. et al. [Evaluation of serum CC-16 as a biomarker for COPD in the ECLIPSE cohort](#). *Thorax*. **63**, 1058-63 (2008).
14. Vestbo, J. et al. Changes in forced expiratory volume in 1 second over time in COPD. *N Engl J Med*. **365**, 1184-92 (2011).
15. Guerra, S. et al. Club cell secretory protein in serum and bronchoalveolar lavage of patients with asthma. *J Allergy Clin Immunol*. **138**, 932-934 (2016).

## Figure Legends

Figure COVID-19 patient lungs exhibit mucus plugs and pathological changes in the airway epithelium. Chest x-ray obtained on January 12, 2020 (**A1**), on January 17, 2020 (**B1**) and on January 22, 2020 (**C1**). Representative lung CT images on January 13, 2020 (**D1**) and (**E1**). Representative transverse lung CT images on January 23, 2020 (**F1**) and (**G1**). Chest x-ray obtained on January 30, 2020 (**H1**), on February 01, 2020 (**I1**) and on February 15, 2020 (**J1**). (**K1**) Representative images of lung tissue sections stained with hematoxylin and eosin from the COVID-19 patient. Asterisks indicate airways. (**L1**) Representative images of lung tissue sections stained with periodic acid-Schiff from the COVID-19 patient. The arrows point to goblet cells. Asterisks indicate mucus plugs in the airways. (**M1**) Immunostaining for MUC5AC (green) and DAPI staining (blue) of sections of larger distal bronchioles from healthy controls (n=3) and the COVID-19 patient. The arrow points to the mucus plug. The arrow head points to the goblet cell. (**N1**) Quantification of the number of larger distal bronchioles plugged by mucus in healthy controls (n=3) and the COVID-19 patient. (**O1**) Quantification of the number of larger distal bronchioles with MUC5AC<sup>+</sup> cells in healthy controls (n=3) and the COVID-19 patient. (**P1**) Immunostaining for MUC5AC (green) and DAPI staining (blue) of sections of the smaller distal bronchioles from healthy controls (n=3) and the COVID-19 patient. The arrow points to the mucus plug. (**Q1**) Quantification of the number of smaller distal bronchioles plugged by mucus in healthy controls (n=3) and the COVID-19 patient. (**R1**) Quantification of the number of smaller distal bronchioles with MUC5AC<sup>+</sup> cells in healthy controls (n=3) and the COVID-19 patient. (**A2**) Relative *MUC5AC* mRNA levels in the lungs from healthy controls and the COVID-19 patient. (**B2**) Immunostaining for MUC5B (red) and DAPI staining (blue) of sections of the airways from healthy controls (n=3) and the COVID-19 patient. (**C2**) Quantification of mean fluorescence intensity of MUC5B immunostaining in the airways in healthy controls (n=3) and the COVID-19 patient. (**D2**) Relative *MUC5B* mRNA levels in the lungs from healthy controls and the COVID-19 patient. (**E2**) Immunostaining for acetylated alpha-tubulin (green) and DAPI staining (blue) of sections of small bronchioles from healthy controls (n=3) and the COVID-19 patient. (**F2**) Quantification of the relative number of acetylated alpha-tubulin<sup>+</sup> multiciliated cells in small bronchioles in healthy controls (n=3) and the COVID-19 patient. (**G2**) Immunostaining for CC16 (red) and DAPI staining (blue) of sections of distal bronchioles from healthy controls (n=3) and the COVID-19 patient. (**H2**) Quantification of the relative number of CC16<sup>+</sup> cells in distal bronchioles in healthy controls (n=3) and the COVID-19 patient. (**I2**) Relative *CC16* mRNA levels in the lungs from healthy controls and the COVID-19 patient. (**J2**) Quantification of CC16 levels in serum from healthy controls (n=7) and severe and critical COVID-19 patients (n=9). (**K2**) Immunostaining for IL-13 (red) and DAPI staining (blue) of sections of the lungs from healthy controls (n=3) and the COVID-19 patient. (**L2**) Quantification of mean fluorescence intensity of IL-13 immunostaining in the lungs in healthy controls (n=3) and the COVID-19 patient. (**M2**) Representative images of cross sections of ALI cultures stained with hematoxylin and eosin. The arrow points to cilia. (**N2**) Trans-epithelial electrical resistance measurements. (**O2**) Immunostaining for MUC5AC (red), SARS-CoV-2 N (green) and DAPI staining (blue) in HBE cells at the ALI after a 14-day differentiation. Scale bars: 100  $\mu$ m (**K1**, **L1**, **M1**, **P1**, **O2**), 20  $\mu$ m (**B2**, **E2**, **G2**, **K2**, **M2**). SARS-CoV-2 N: SARS-CoV-2 nucleocapsid proteins. \**P* < 0.05; \*\**P* < 0.01; \*\*\**P* < 0.001; \*\*\*\**P* < 0.0001; Unpaired Student's *t*-test, mean  $\pm$  s.d.



Yin et al., Fig. 2.